PERGAMON

International Journal of Multiphase Flow 26 (2000) 1509–1524

International Journal of Multiphase Flow

www.elsevier.com/locate/ijmulflow

A new formulation of the distributed Lagrange multiplier/fictitious domain method for particulate flows

N.A. Patankar[a,*], P. Singh[b], D.D. Joseph[a], R. Glowinski[c], T.-W. Pan[c]

[a] *Department of Aerospace Engineering and Mechanics, University of Minnesota, Minneapolis, MN 55455, USA*
[b] *Department of Mechanical Engineering, NJIT, University Heights, Newark, NJ 07102, USA*
[c] *Department of Mathematics, University of Houston, Houston, TX 77204, USA*

Received 20 April 1999; received in revised form 7 September 1999

Abstract

A Lagrange-multiplier-based fictitious-domain method (DLM) for the direct numerical simulation of rigid particulate flows in a Newtonian fluid was presented previously. An important feature of this finite element based method is that the flow in the particle domain is constrained to be a rigid body motion by using a well-chosen field of Lagrange multipliers. The constraint of rigid body motion is represented by $\boldsymbol{u} = \boldsymbol{U} + \boldsymbol{\omega} \times \boldsymbol{r}$; $\boldsymbol{u}$ being the velocity of the fluid at a point in the particle domain; $\boldsymbol{U}$ and ω are the translational and angular velocities of the particle, respectively; and $\boldsymbol{r}$ is the position vector of the point with respect to the center of mass of the particle. The fluid–particle motion is treated implicitly using a combined weak formulation in which the mutual forces cancel. This formulation together with the above equation of constraint gives an algorithm that requires extra conditions on the space of the distributed Lagrange multipliers when the density of the fluid and the particles match. In view of the above issue a new formulation of the DLM for particulate flow is presented in this paper. In this approach the deformation rate tensor within the particle domain is constrained to be zero at points in the fluid occupied by rigid solids. This formulation shows that the state of stress inside a rigid body depends on the velocity field similar to pressure in an incompressible fluid. The new formulation is implemented by modifying the DLM code for two-dimensional particulate flows developed by others. The code is verified by comparing results with other simulations and experiments.

Keywords: Distributed Lagrange multiplier/fictitious domain method; Finite element method; Direct numerical simulation; Particulate flow; Solid–liquid flow; Viscoelastic fluid; Operator splitting; Rigidity constraint

* Corresponding author.

0301-9322/00/$ - see front matter
PII: S0301-9322(99)00100-7

1. Introduction

Direct numerical simulation of the motion of rigid bodies in a fluid can be applied in numerous settings; e.g. sedimenting and fluidized suspensions, lubricated transport, hydraulic fracturing of reservoirs, slurries etc. The capability of simulating the motion of large numbers of particles in a fluid is important for predicting the effective properties of the particulate mixture in such applications.

Hu et al. (1992), Hu (1996) and Johnson and Tezduyar (1996, 1997) developed finite element methods based on unstructured grids to simulate the motion of large numbers of rigid particles in two and three dimensions in a Newtonian fluid. Hu (1996) treats the fluid–particle motion implicitly by using a combined weak formulation of Hesla (1991). The method of Hu et al. (1992) for a Newtonian suspending fluid was first extended for static simulation of particles in a viscoelastic fluid by Huang and Feng (1995). The same scheme was later extended by them to enable dynamic simulation of particles, the first results of which were presented by Feng et al. (1996). Hu (1996) further improved their scheme. Recent results of dynamic simulation of particles in a viscoelastic fluid can be found in the papers by Huang et al. (1997, 1998). Their numerical scheme has been described in detail by Patankar (1997) and the simulation results for about 100 particles in two dimensions in an Oldroyd-B fluid were also reported there.

Glowinski et al. (1999, 1998) presented a Lagrange-multiplier-based fictitious-domain method (DLM) for the direct numerical simulation of the motion of large numbers of rigid particles in a Newtonian fluid. Their finite element formulation permits the use of a fixed structured grid. This eliminates the need for remeshing the domain which is necessary in the unstructured grid based methods. Structured grids also allow the use of fast and efficient solvers. A recent three-dimensional calculation of the fluidization of 1204 spheres by Pan can be found at the web site http://www.aem.umn.edu/Solid-Liquid_Flows. Singh et al. (1999) extended this method to simulate the motion of rigid particles in an Oldroyd-B fluid.

In the DLM method the flow in the particle domain is constrained to be a rigid body motion using a field of Lagrange multipliers. The constraint of rigid body motion is represented by

$$\boldsymbol{u} = \boldsymbol{U} + \boldsymbol{\omega} \times \boldsymbol{r}, \tag{1}$$

$\boldsymbol{u}$ being the velocity of the fluid at a point in the particle domain; $\boldsymbol{U}$ and $\boldsymbol{\omega}$ are the translational and angular velocities of the particle, respectively; and $\boldsymbol{r}$ is the position vector of the point with respect to the center of mass of the particle. The fluid–particle motion is treated implicitly using a combined weak formulation of Hesla (1991) in which the mutual forces cancel. This formulation and the above equation of constraint were the key features of the DLM method of Glowinski et al. (1999). They stated that the resulting algorithm as presented by them could not be used directly if the particles were neutrally buoyant; however, it could be made to work by adding extra conditions to the space of the distributed Lagrange multipliers. Extension of this formulation to three dimensions with irregularly shaped bodies requires that another term ($\boldsymbol{\omega} \times \boldsymbol{I}_{\mathrm{p}}\boldsymbol{\omega}$, where $\boldsymbol{I}_{\mathrm{p}}$ is the moment of inertia tensor) must be added to the angular momentum equation for particles in the coupled particle–fluid system of equation.

In this paper, we address the above issues by presenting a new DLM formulation for particulate flow. It was recognized by Hesla (1997) that, in the DLM method of Glowinski et

al. (1999) the translational and angular velocities of the particles appear as "extra unknowns", in some sense, in addition to the velocity field $\boldsymbol{u}$ inside the particles, even though they are completely determined in terms of $\boldsymbol{u}$. Hence, he suggested that $\boldsymbol{U}$ and $\boldsymbol{\omega}$ be eliminated as independent unknowns at the outset by replacing them by the respective classical mechanical integral expressions in terms of $\boldsymbol{u}$. This suggestion if implemented gives rise to an algorithm that can be used in the density matched case without extra conditions on the space of the distributed Lagrange multipliers. In this paper we present an approach in which the deformation rate tensor within the particle domain is constrained to be zero in order to impose the rigid body motion. This eliminates $\boldsymbol{U}$ and $\boldsymbol{\omega}$ as variables from the coupled system of equations and at the same time is much easier to implement, numerically, compared to the suggestion of Hesla (1997). The resulting algorithm in our approach requires no extra conditions for the density matched case. Physical interpretation of the formulation will be explained in the next section. We will then present some details of the numerical implementation of the new formulation. We implemented this formulation by modifying the DLM code for two-dimensional particulate flows developed by Singh et al. (1999). Finally, we will verify the code through some known test cases.

2. Mathematical formulation

2.1. Strong form

Let Ω be the computational domain which includes both the fluid and the particle domain. Let $P(t)$ be the particle domain. Let the fluid boundary not shared with the particle be denoted by Γ. For simplicity we will assume that a Dirichlet boundary condition is imposed on Γ and that there is only one particle in the computational domain. We note that the formulation can be easily generalized beyond these assumptions. The body force will also be assumed to be constant so that there is no net torque acting on the particles. The governing equations for fluid motion are given by:

$$\rho_{\mathrm{f}}\left(\frac{\partial \boldsymbol{u}}{\partial t}+(\boldsymbol{u}\cdot\nabla)\boldsymbol{u}\right)=\nabla\cdot\boldsymbol{\sigma}+rho_{\mathrm{f}}\boldsymbol{g}\quad\text{in } \Omega\backslash\overline{P(t)}, \tag{2}$$

$$\nabla\cdot\boldsymbol{u}=0\quad\text{in } \Omega\backslash\overline{P(t)}, \tag{3}$$

$$\boldsymbol{u}=\boldsymbol{u}_{\Gamma}(t)\quad\text{on } \Gamma, \tag{4}$$

$$\boldsymbol{u}=\boldsymbol{u}_i\quad\text{on } \partial P(t), \tag{5a}$$

$$\boldsymbol{\sigma}\cdot\boldsymbol{n}=\boldsymbol{t}\quad\text{on } \partial P(t), \tag{5b}$$

$$\boldsymbol{u}|_{t=0}=\boldsymbol{u}_0(\boldsymbol{x})\quad\text{in } \Omega\backslash\overline{P(0)}, \tag{6}$$

where ρ_f is the fluid density, $\boldsymbol{u}$ is the fluid velocity, $\boldsymbol{g}$ is the acceleration due to gravity, $\boldsymbol{n}$ is the outward normal on the particle surface, $\boldsymbol{u}_i$ is the velocity at fluid–particle interface $\partial P(t)$ and $\boldsymbol{\sigma}$ is the stress tensor. The initial velocity $\boldsymbol{u}_0$ should satisfy Eq. (3). The boundary velocity in Eq. (4) should satisfy the compatibility condition due to Eq. (3). For an incompressible fluid the divergence-free constraint (3) gives rise to pressure in the fluid. The stress tensor is then given by:

$$\boldsymbol{\sigma} = -p\boldsymbol{I} + \boldsymbol{\tau}, \tag{7}$$

where $\boldsymbol{I}$ is the identity tensor, p is the pressure and $\boldsymbol{\tau}$ is the extra stress tensor. For a Newtonian fluid, $\boldsymbol{\tau}$ represents the viscous stress, whereas for a viscoelastic fluid it represents the viscous and the elastic stress in the fluid. Extra stress depends on the deformation rate of the fluid at a given location. In a viscoelastic fluid it also depends on the history of deformation.

Particle motions can be represented in terms of translational and angular velocities using Newton's second law. In the present formulation, we treat the particle as a fluid subjected to an additional rigidity constraint. The governing equations for particle motion are then given by:

$$\rho_s\left(\frac{\partial \boldsymbol{u}}{\partial t} + (\boldsymbol{u}\cdot\nabla)\boldsymbol{u}\right) = \nabla\cdot\boldsymbol{\sigma} + \rho_s\boldsymbol{g} \quad \text{in } P(t), \tag{8}$$

$$\nabla\cdot\boldsymbol{u} = 0 \quad \text{in } P(t), \tag{9}$$

$$\boldsymbol{D}[\boldsymbol{u}] = \frac{1}{2}\left(\nabla\boldsymbol{u} + \nabla\boldsymbol{u}^{\mathrm{T}}\right) = \boldsymbol{0} \quad \text{in } P(t), \tag{10}$$

$$\boldsymbol{u} = \boldsymbol{u}_i \quad \text{on } \partial P(t), \tag{11a}$$

$$\boldsymbol{\sigma}\cdot\boldsymbol{n} = \boldsymbol{t} \quad \text{on } \partial P(t), \tag{11b}$$

$$\boldsymbol{u}|_{t=0} = \boldsymbol{u}_0(\boldsymbol{x}) \quad \text{in } P(0), \tag{12}$$

where ρ_s is the particle density. Rigidity constraint (10) has been used before by Joseph and Lundgren (1990) to derive the ensemble averaged two-fluid equations for flowing composites of solid particles in a liquid. The initial velocity $\boldsymbol{u}_0$ should satisfy Eq. (10). The rigidity constraint (10) ensures that the velocity field is divergence-free. Hence, Eq. (9) is a redundant equation. We nevertheless choose to keep this constraint since it will be required in the DLM formulation to be presented later. As noted earlier, Eq. (9) gives rise to a pressure field in the particle domain. Similarly, the rigidity constraint (which is a tensor constraint) gives rise to a stress field $\boldsymbol{L}$ (which is a symmetric second-order tensor). Variational analysis of the above equations shows that the pressure and $\boldsymbol{L}$ are nothing but distributed Lagrange multipliers due to the divergence-free and rigidity constraints, respectively. This will become evident in the weak form to be presented in the next section. $\boldsymbol{L}$ is an additional stress field required inside the particle domain to maintain the rigid-body motion. A similar interpretation of the Lagrange

multiplier in terms of additional body force per unit volume was given by Glowinski et al. (1999). Stress inside the particle is then given by:

$$\boldsymbol{\sigma} = -p\boldsymbol{I} + \boldsymbol{L} + \boldsymbol{\tau}. \tag{13}$$

$\boldsymbol{\tau}$ can considered to be zero inside the particle domain since the deformation inside a rigid particle is always zero. The pressure term will not arise if Eq. (9) is not used.

On using Eq. (10) to apply the rigidity constraint we obtain a Lagrange multiplier $\boldsymbol{L}$ with six scalar variables in the three-dimensional case. This is because Eq. (10) represents six scalar constraint equations at a point. A reformulation of Eq. (10) can reduce the number of Lagrange multiplier variables to three. To this end we note that rigidity constraint can also be implemented by imposing:

$$\nabla \cdot (\boldsymbol{D}[\boldsymbol{u}]) = \boldsymbol{0} \quad \text{in } P(t), \tag{14}$$

$$\boldsymbol{D}[\boldsymbol{u}] \cdot \boldsymbol{n} = \boldsymbol{0} \quad \text{on } \partial P(t), \tag{15}$$

where (14) and (15) represent the three scalar constraint equations at a point. As a result $\boldsymbol{L}$ is no longer the Lagrange multiplier itself. It remains the stress field inside the particle due to the rigidity constraint. It can be represented in terms of a Lagrange multiplier $\boldsymbol{\lambda}$ by an expression to be derived in the next section. The expression is

$$\boldsymbol{L} = \boldsymbol{D}[\boldsymbol{\lambda}], \tag{16}$$

where $\boldsymbol{\lambda}$ is a vector with three scalar components in a three-dimensional case.

The idea of computing the motion inside the particle as a (rigid) velocity field $\boldsymbol{u}$ produced by a certain (symmetric) stress tensor field $\boldsymbol{\sigma}$ was proposed by Hesla (1995). In Hesla's method, the entire stress tensor $\boldsymbol{\sigma}$ inside the particle is postulated as $\boldsymbol{D}[\boldsymbol{\phi}]$, where $\boldsymbol{\phi}$ is an unknown vector field satisfying the inhomogeneous equation (23), to be presented later, with $\boldsymbol{\lambda}$ replaced by $\boldsymbol{\phi}$. A finite-element code implementing Hesla's method is currently under development. We note that in the present approach the form for stress inside a rigid solid given by Eq. (16) is an outcome of the rigidity constraint (Eqs. (14) and (15)) and is not postulated as in the approach of Hesla (1995). This derivation will be presented next.

2.2. Weak form

In the following derivation we will consider the two-dimensional case. To obtain the weak form of the governing equations of the fluid we use the traction boundary condition on the fluid–particle interface. We define the solution space for velocity in the fluid domain as

$$V_{u\Gamma}(t) = \left\{ \boldsymbol{u} | \boldsymbol{u} \in H^1\left(\Omega \backslash \overline{P(t)}\right)^2, \boldsymbol{u} = \boldsymbol{u}_\Gamma(t) \text{ on } \Gamma \right\}$$

and the variation space for the velocity as

$$V_0(t) = \left\{ \boldsymbol{v} | \boldsymbol{v} \in H^1\left(\Omega \backslash \overline{P(t)}\right)^2, \boldsymbol{v} = \boldsymbol{0} \text{ on } \Gamma \right\}.$$

The solution space for pressure is

$$L_0^2\left(\Omega\backslash\overline{P(t)}\right) = \left\{ q \in L^2\left(\Omega\backslash\overline{P(t)}\right) | \int_{\Omega\backslash\overline{P(t)}} q \, \mathbf{dx} = 0 \right\}.$$

The weak formulation for the fluid phase is:

$$\begin{aligned} &\int_{\Omega\backslash\overline{P(t)}} \rho_f \left(\frac{\partial \boldsymbol{u}}{\partial t} + (\boldsymbol{u}\cdot\nabla)\boldsymbol{u} - \boldsymbol{g} \right) \cdot \boldsymbol{v} \, \mathbf{dx} + \int_{\Omega\backslash\overline{P(t)}} \boldsymbol{\sigma}:\boldsymbol{D}[\boldsymbol{v}] \, \mathbf{dx} + \int_{\partial P(t)} (\boldsymbol{\sigma}\cdot\boldsymbol{n})\cdot\boldsymbol{v} \, \mathbf{dx} \\ &\quad + \int_{\Omega\backslash\overline{P(t)}} q(\nabla\cdot\boldsymbol{u}) \, \mathbf{dx} = 0, \quad \forall \boldsymbol{v} \in V_0 \text{ and } q \in L^2\left(\Omega\backslash\overline{P(t)}\right). \end{aligned} \tag{17}$$

To obtain the weak form of the particle equations we use the traction boundary condition as before. As a first step we impose the rigidity constraint in the solution and variation space for velocity in the particle domain. It is given by

$$V_P(t) = \left\{ \boldsymbol{v} | \boldsymbol{v} \in H^1(P(t))^2, \boldsymbol{D}[\boldsymbol{v}] = \boldsymbol{0} \text{ in } P(t) \right\}.$$

For $\boldsymbol{u} \in V_P(t)$ and $p \in L_0^2(P(t))$ the weak formulation for the particle phase becomes:

$$\begin{aligned} &\int_{P(t)} \rho_s \left[\frac{\partial \boldsymbol{u}}{\partial t} + (\boldsymbol{u}\cdot\nabla)\boldsymbol{u} - \boldsymbol{g} \right] \cdot \boldsymbol{v} \, \mathbf{dx} - \int_{P(t)} p(\nabla\cdot\boldsymbol{v}) \, \mathbf{dx} - \int_{\partial P(t)} (\boldsymbol{\sigma}\cdot\boldsymbol{n})\cdot\boldsymbol{v} \, \mathbf{dx} \\ &\quad + \int_{P(t)} q(\nabla\cdot\boldsymbol{u}) \, \mathbf{dx} = 0, \quad \forall \boldsymbol{v} \in V_P \text{ and } q \in L^2(P(t)). \end{aligned} \tag{18}$$

As in the approach of Glowinski et al. (1999) we relax the constraint in the velocity space $V_P(t)$ by enforcing it in a weak sense as a side constraint. The weak form of the constraint equation can be taken to be the weak form of Eqs. (14) and (15). It is given by

$$\int_{P(t)} \boldsymbol{D}[\boldsymbol{\mu}]:\boldsymbol{D}[\boldsymbol{u}] \, \mathrm{d}\boldsymbol{x} = 0, \quad \forall \boldsymbol{\mu} \in H^1(P(t))^2, \tag{19}$$

where $\boldsymbol{u} \in H^1(P(t))^2$. Using Eq. (19) requires the addition of an appropriate distributed Lagrange multiplier $\boldsymbol{\lambda}$ in Eq. (18). The modified weak formulation for the particle phase becomes

$$\begin{aligned} &\int_{P(t)} \rho_s \left(\frac{\partial \boldsymbol{u}}{\partial t} + (\boldsymbol{u}\cdot\nabla)\boldsymbol{u} - \boldsymbol{g} \right) \cdot \boldsymbol{v} \, \mathbf{dx} - \int_{P(t)} p(\nabla\cdot\boldsymbol{v}) \, \mathbf{dx} + \int_{P(t)} \boldsymbol{D}[\boldsymbol{\lambda}]:\boldsymbol{D}[\boldsymbol{v}] \, \mathbf{dx} - \int_{\partial P(t)} (\boldsymbol{\sigma}\cdot\boldsymbol{n})\cdot\boldsymbol{v} \, \mathbf{dx} \\ &\quad + \int_{P(t)} q(\nabla\cdot\boldsymbol{u}) \, \mathbf{dx} + \int_{P(t)} \boldsymbol{D}[\boldsymbol{\mu}]:\boldsymbol{D}[\boldsymbol{u}] \, \mathbf{dx} = 0, \quad \forall \boldsymbol{v} \in H^1(P(t))^2, \boldsymbol{\mu} \in H^1(P(t))^2 \\ &\quad \text{and } q \in L^2(P(t)), \end{aligned} \tag{20}$$

where $\boldsymbol{u} \in H^1(P(t))^2$, $\boldsymbol{\lambda} \in H^1(P(t))^2$ and $p \in L_0^2(P(t))$. It can be verified that the strong form of Eq. (20) is represented by Eqs. (8)–(10) and (13)–(16). As stated before, Eq. (16) is obtained due

the imposition of rigidity constraint (19). Physically one may perceive the stress $\boldsymbol{L}$ in a rigid body to be similar to pressure in an incompressible fluid. In the DLM formulation of Glowinski et al. (1999) various forms of constraint equations were suggested. For the present formulation we see that Eq. (19) is the most suitable form of the constraint equation.

Adding Eqs. (17) and (20), using the interface conditions (5) and (11) and noting that the extra stress $\boldsymbol{\tau}$ (modeled as a function of the deformation rate or the deformation history) is zero inside a rigid body we get the following combined weak form of the problem:

For $t > 0$, find $\boldsymbol{u} \in W_{u\Gamma}$, $p \in L_0^2(\Omega)$, $\boldsymbol{\lambda} \in H^1(P(t))^2$ satisfying

$$\begin{aligned}&\int_\Omega \rho_f\left(\frac{\partial \boldsymbol{u}}{\partial t} + (\boldsymbol{u}\cdot\nabla)\boldsymbol{u} - \boldsymbol{g}\right)\cdot \boldsymbol{v}\,\mathrm{d}\boldsymbol{x} - \int_\Omega p(\nabla\cdot\boldsymbol{v})\,\mathrm{d}\boldsymbol{x} + \int_\Omega q(\nabla\cdot\boldsymbol{u})\,\mathrm{d}\boldsymbol{x} + \int_\Omega \boldsymbol{\tau}:\boldsymbol{D}[\boldsymbol{v}]\,\mathrm{d}\boldsymbol{x}\\ &+ \int_{P(t)} (\rho_s - \rho_f)\left(\frac{\partial \boldsymbol{u}}{\partial t} + (\boldsymbol{u}\cdot\nabla)\boldsymbol{u} - \boldsymbol{g}\right)\cdot \boldsymbol{v}\,\mathrm{d}\boldsymbol{x} + \int_{P(t)} \boldsymbol{D}[\boldsymbol{\lambda}]:\boldsymbol{D}[\boldsymbol{v}]\,\mathrm{d}\boldsymbol{x} + \int_{P(t)} \boldsymbol{D}[\boldsymbol{\mu}]:\boldsymbol{D}[\boldsymbol{u}]\,\mathrm{d}\boldsymbol{x}\\ &= 0, \quad \forall \boldsymbol{v} \in W_0,\ \boldsymbol{\mu} \in H^1(P(t))^2 \text{ and } q \in L^2(\Omega),\end{aligned} \tag{21}$$

where

$$W_{u\Gamma}(t) = \left\{\boldsymbol{v} | \boldsymbol{v} \in H^1(\Omega)^2,\ \boldsymbol{v} = \boldsymbol{u}_\Gamma(t) \text{ on } \Gamma\right\},$$

$$W_0(t) = \left\{\boldsymbol{v} | \boldsymbol{v} \in H^1(\Omega)^2,\ \boldsymbol{v} = \boldsymbol{0} \text{ on } \Gamma\right\},$$

$$L_0^2(\Omega) = \left\{q \in L^2(\Omega) | \int_\Omega q\,\boldsymbol{dx} = 0\right\}.$$

The initial conditions are given by Eqs. (6) and (12). The fluid–particle interface condition is internal to the combined system. Hence, there are no explicit interface force or velocity terms in Eq. (21). We note that the particle translational and angular velocities are not present in the combined form (21) unlike the original DLM formulation of Glowinski et al. (1999). This is especially convenient in a three-dimensional case with irregularly shaped bodies for which there is added complexity due to the nonlinear nature of the angular momentum equations. The above formulation is due to the first author.

2.3. An alternate strong form

The third author has proposed that one can rewrite the strong form presented in Section 2.1 for given velocity and position of the particles. We can extract the following problems for $\boldsymbol{u}$ and $\boldsymbol{\lambda}$ on $\Omega\backslash\overline{P(t)}$ and $P(t)$, given $\boldsymbol{U}(t)$ and $\boldsymbol{\omega}(t)$ and the translational and angular positions of the particles:

$$\rho_f\left(\frac{\partial \boldsymbol{u}}{\partial t} + (\boldsymbol{u}\cdot\nabla)\boldsymbol{u}\right) = -\nabla p + \nabla\cdot\boldsymbol{\tau} + \rho_f \boldsymbol{g} \quad \text{in } \Omega\backslash\overline{P(t)},$$

$$\nabla \cdot \boldsymbol{u} = 0 \quad \text{in } \Omega \backslash \overline{P(t)},$$

$$\boldsymbol{u} = \boldsymbol{u}_\Gamma(t) \quad \text{on } \Gamma,$$

$$\boldsymbol{u} = \boldsymbol{U} + \boldsymbol{\omega} \times \boldsymbol{r} \quad \text{on } \partial P(t) \tag{22}$$

and

$$\nabla \cdot \left[\boldsymbol{D}(\boldsymbol{\lambda})\right] = \rho_s \left(\frac{\mathrm{d}\boldsymbol{U}}{\mathrm{d}t} + \frac{\mathrm{d}\boldsymbol{\omega}}{\mathrm{d}t} \times \boldsymbol{r} + \boldsymbol{\omega} \times (\boldsymbol{\omega} \times \boldsymbol{r}) - \boldsymbol{g} \right) \quad \text{in } P(t),$$

$$\boldsymbol{n} \cdot \left[\boldsymbol{D}(\boldsymbol{\lambda})\right]_s = \boldsymbol{n} \cdot [-p\boldsymbol{I} + \boldsymbol{\tau}]_f \quad \text{on } \partial P(t), \tag{23}$$

where we have not defined pressure in the particle domain since it is redundant in the presence of stress due to $\boldsymbol{\lambda}$, and $\boldsymbol{\tau}$ in the particle domain is taken to be zero. Thus the stress in the particle is only due to the Lagrange multiplier $\boldsymbol{\lambda}$. We have used Eq. (1) in order to derive Eq. (23) from Eq. (8). In the second part of Eq. (23), the left-hand side is evaluated in the particle domain and the right-hand side is evaluated in the fluid domain. Initial conditions are the same as given before. These are solvable Dirichlet and Neumann problems which are decoupled for any specified motion of the particles. The strong form in Eqs. (22) and (23) can form a basis for a new computational scheme. In such a scheme the fluid domain can be extended to include the particle domain. Eq. (23) then ensures that the region occupied by the particles move rigidly. Hesla's (Hesla, 1995) scheme, mentioned earlier, is based on essentially the same set of strong equations. In the present work, the above strong form is not considered in the numerical implementation.

3. Numerical scheme

The new formulation is implemented by modifying the DLM code for two-dimensional particulate flows developed by Singh et al. (1999). Their code can simulate rigid particulate flows in Newtonian as well as viscoelastic fluids. To highlight the modification of their code we will consider the suspending fluid to be Newtonian. The particles are assumed to be circular so that the angular motion of the particles need not be considered. Singh et al. (1999) use the Marchuk–Yanenko operator splitting scheme for time discretization. The modified algorithm based on this scheme is:

1. Calculate particle velocity: Given $\boldsymbol{u}^n$ and $P(t^n)$, find the translational velocity, $\boldsymbol{U}^n$, of the particle:

$$\boldsymbol{U}^n = \frac{1}{M} \int_{P(t^n)} \rho_s \boldsymbol{u}^n \, \mathrm{d}\boldsymbol{x}, \tag{24a}$$

where M is the mass of the particle. For a non-circular particle it is necessary to update the angular position of the particle. Angular velocity, $\boldsymbol{\omega}^n$, of the particle is then calculated by

$$\boldsymbol{I}_{\mathrm{p}}\boldsymbol{\omega}^{n}=\int_{P(t^{n})}\boldsymbol{r}\times\rho_{\mathrm{s}}\boldsymbol{u}^{n}\,\mathrm{d}\boldsymbol{x}, \tag{24b}$$

where $\boldsymbol{I}_{\mathrm{p}}$ is the moment of inertia of the particle.

2. Explicit update of particle position: Compute $\boldsymbol{X}^{n+1}$ by the following procedure:
   Set $\boldsymbol{X}^{n+1,\,0}=\boldsymbol{X}^{n}$.
   do $k=1, K$

$$\boldsymbol{X}^{*n+1,\,k}=\boldsymbol{X}^{n+1,\,k-1}+\left(\frac{\boldsymbol{U}^{n}+\boldsymbol{U}^{n-1}}{2}\right)\left(\frac{\Delta t}{K}\right) \tag{25}$$

$$\boldsymbol{X}^{n+1,\,k}=\boldsymbol{X}^{*n+1,\,k}+M^{-1}\left(\frac{\boldsymbol{F}(\boldsymbol{X}^{n+1,\,k-1})+\boldsymbol{F}(\boldsymbol{X}^{*n+1,\,k})}{2}\right)\frac{(\Delta t)^{2}}{2K^{2}} \tag{26}$$

   enddo
   Set $\boldsymbol{X}^{n+1}=\boldsymbol{X}^{n+1,\,K}$, this also gives $P(t^{n+1})$.
   Set

$$\boldsymbol{A}_{\mathrm{c}}^{n+1}=\frac{2}{(\Delta t)^{2}}\left(\boldsymbol{X}^{n+1}-\boldsymbol{X}^{n}-\left(\frac{\boldsymbol{U}^{n}+\boldsymbol{U}^{n-1}}{2}\right)\Delta t\right), \tag{27}$$

   where $\boldsymbol{F}$ denotes the collision force acting on the particles to prevent them from penetrating each other or the walls of the domain. Modeling of this force in the present scheme is the same as that of Glowinski et al. (1999). More details can be found therein. $\boldsymbol{A}_{\mathrm{c}}$ is the acceleration of the particle due to collision. This term provides an additional body force acting on the particle and is included in the combined momentum equation to be solved in the subsequent steps. This explicit update scheme is similar although not identical to that used by Hu (1996) in the present version of his code. In his scheme the calculation of $\boldsymbol{F}$ is done differently. Glowinski et al. (1999) and Singh et al. (1999) did not use explicit update scheme.

3. Fractional step 1: Find $\boldsymbol{u}^{n+1/3}\in W_{u\Gamma}(t^{n+1})$ and $p^{n+1/3}\in L_{0}^{2}(\Omega)$ satisfying

$$\begin{aligned}&\int_{\Omega}\rho_{\mathrm{f}}\left(\frac{\boldsymbol{u}^{n+1/3}-\boldsymbol{u}^{n}}{\Delta t}-\boldsymbol{g}\right)\cdot\boldsymbol{v}\,\mathrm{d}\boldsymbol{x}-\int_{\Omega}p^{n+1/3}(\nabla\cdot\boldsymbol{v})\,\mathrm{d}\boldsymbol{x}+\int_{\Omega}q(\nabla\cdot\boldsymbol{u}^{n+1/3})\,\mathrm{d}\boldsymbol{x}\\&\quad+\alpha\int_{\Omega}2\eta\boldsymbol{D}[\boldsymbol{u}^{n+1/3}]{:}\boldsymbol{D}[\boldsymbol{v}]\,\mathrm{d}\boldsymbol{x}=0,\quad\forall\boldsymbol{v}\in W_{0}\text{ and }q\in L^{2}(\Omega).\end{aligned} \tag{28}$$

4. Fractional step 2: Find $\boldsymbol{u}^{n+2/3}\in W_{u\Gamma}(t^{n+1})$ satisfying

$$\begin{aligned}&\int_{\Omega}\rho_{\mathrm{f}}\left(\frac{\boldsymbol{u}^{n+2/3}-\boldsymbol{u}^{n+1/3}}{\Delta t}+(\boldsymbol{u}^{n+2/3}\cdot\nabla)\boldsymbol{u}^{n+2/3}\right)\cdot\boldsymbol{v}\,\mathrm{d}\boldsymbol{x}+\beta\int_{\Omega}2\eta\boldsymbol{D}[\boldsymbol{u}^{n+2/3}]{:}\boldsymbol{D}[\boldsymbol{v}]\,\mathrm{d}\boldsymbol{x}=0,\\&\forall\boldsymbol{v}\in W_{0}.\end{aligned} \tag{29}$$

5. Fractional step 3: Find $\boldsymbol{u}^{n+1} \in W_{u\Gamma}(t^{n+1})$ and $\boldsymbol{\lambda}^{n+1} \in H^1[P(t^{n+1})]^2$ satisfying

$$\int_\Omega \rho_f \left(\frac{\boldsymbol{u}^{n+1} - \boldsymbol{u}^{n+2/3}}{\Delta t} \right) \cdot \boldsymbol{v}\, \mathrm{d}\boldsymbol{x} + \gamma \int_\Omega 2\eta \boldsymbol{D}[\boldsymbol{u}^{n+1}] : \boldsymbol{D}[\boldsymbol{v}]\, \mathrm{d}\boldsymbol{x} - \int_{P(t^{n+1})} \rho_s \boldsymbol{A}_c^{n+1} \cdot \boldsymbol{v}\, \mathrm{d}\boldsymbol{x}$$
$$+ \int_{P(t^{n+1})} \boldsymbol{D}[\boldsymbol{\lambda}^{n+1}] : \boldsymbol{D}[\boldsymbol{v}]\, \mathrm{d}\boldsymbol{x} + \int_{P(t^{n+1})} \boldsymbol{D}[\boldsymbol{\mu}] : \boldsymbol{D}[\boldsymbol{u}^{n+1}]\, \mathrm{d}\boldsymbol{x} + \int_{P(t^{n+1})} (\rho_s - \rho_f) \left(\frac{\boldsymbol{u}^{n+1} - \boldsymbol{u}^n}{\Delta t} \right. \tag{30}$$
$$\left. + (\boldsymbol{u}^{n+2/3} \cdot \nabla) \boldsymbol{u}^{n+2/3} - \boldsymbol{g} \right) \cdot \boldsymbol{v}\, \mathrm{d}\boldsymbol{x} = 0, \quad \forall \boldsymbol{v} \in W_0 \text{ and } \boldsymbol{\mu} \in H^1\left[P(t^{n+1})\right]^2.$$

$\boldsymbol{\tau}$ is replaced by the Newtonian stress and is split into the three fractional steps such that $\alpha + \beta + \gamma = 1$. In our simulations we set $\alpha = \beta = 0.5, \gamma = 0$ and viscosity of the Newtonian fluid is constant. We use linear interpolation for projection between the fluid and particle meshes which is necessary in the last fractional step. The above is a first-order time discretization scheme. In case of a viscoelastic suspending fluid the above algorithm can be extended as per the details provided by Singh et al. (1999). In the present work the viscoelastic fluid model has been implemented. The first fractional step is the classical Stokes-like problem and is solved using a conjugate gradient method. Note that it is essential to have a pressure variable in the particle domain to get the classical Stokes problem in this step. This explains why constraint (9) was retained in the particle equations although it was redundant in the presence of the rigidity constraint. Fractional step two defines a nonlinear problem for velocity which is solved by using a least squares conjugate gradient algorithm. For details of these methods see Bristeau et al. (1987). Fractional step three is solved by a Uzawa conjugate gradient algorithm similar to that used by Glowinski et al. (1999). Details of this will not be repeated here.

We see from Eq. (30) that the algorithm as presented can also be used when the fluid and particle densities match. The above system of equations has been solved by using the Galerkin finite element method. A structured triangular finite element mesh is used, where the pressure is defined on a "twice-coarser" mesh. Linear shape functions are used (see Glowinski et al., 1999 or Singh et al., 1999 for details). A separate mesh, on which the Lagrange multiplier is defined, is used within the particle domain. Glowinski et al. (1999) had mentioned that in their DLM formulation a particle mesh that is coarser than the velocity mesh was good for stability or enhancing the conditioning of the algebraic system. They reported that this followed from general results on the approximation of generalized saddle-point problems. Although it is likely that the present formulation is subject to similar conditions, a comparison of the stability behavior of the present formulation and the pervious DLM formulation needs to be done. In this work we have chosen to use the same coarse mesh in the particle domain as that used by Singh et al. (1999). Use of a particle mesh of the same size as that of velocity can enhance the accuracy of the solution inside and near the particle domain. We intend to study the stability of this formulation under such condition in future. There is no additional computational cost in the present formulation as compared to the previous formulation.

4. Results

We will validate the code by presenting results of sedimentation of two circular particles in a Newtonian fluid. We consider a channel 2 cm wide (x-direction) and 8 cm tall (y-direction). The fluid viscosity is 0.01 g/cm s and the density is 1 g/cm^3. The particle density is 1.01 g/cm^3 and their radius is 0.1 cm. Gravity acts in the negative y-direction. The simulation is started at $t = 0$ s by dropping the two particles at the center of the channel at a height of 7.2 and 6.8 cm. We perform simulations at two different time step and for two different mesh sizes. This case is identical to the one presented by Singh et al. (1999).

It is known that two particles dropped close to each other in a Newtonian fluid will undergo drafting, kissing and tumbling (Fortes et al., 1987). Numerical results in Fig. 1 agree well with

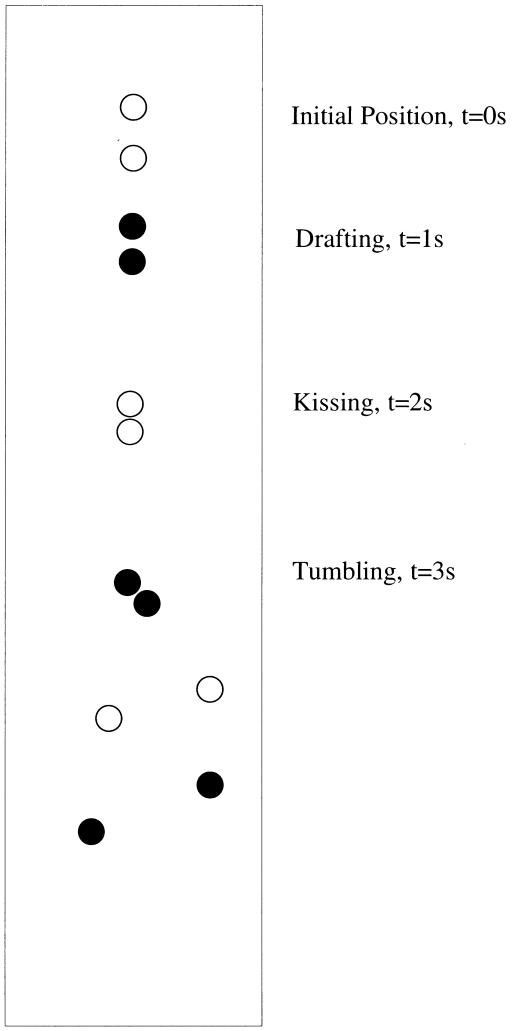

Fig. 1. Numerical simulation of drafting, kissing and tumbling of particles sedimenting in a Newtonian fluid.

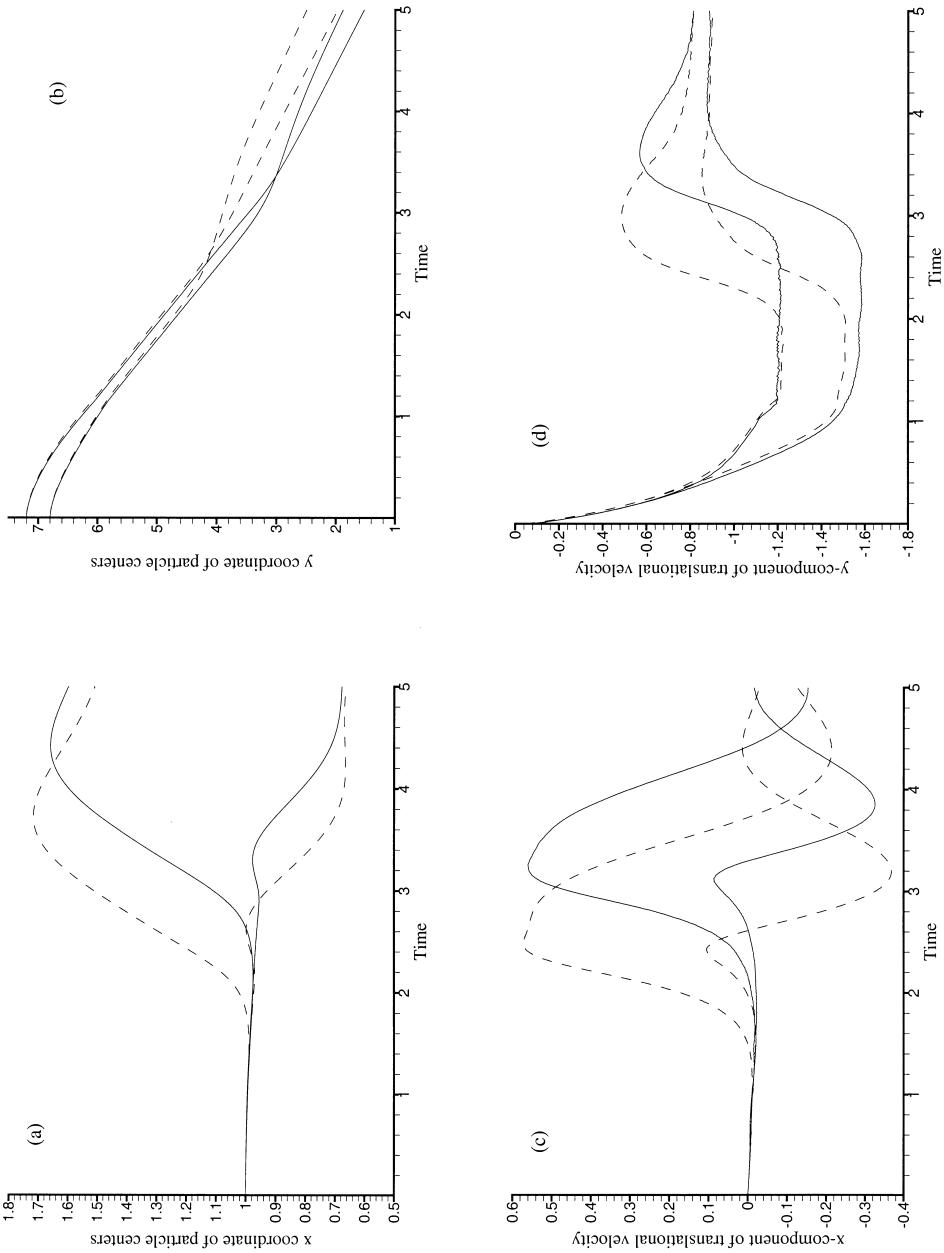

Fig. 2. Time history of (a) x-coordinate of particle centers, (b) y-coordinate of particle centers, (c) x-component of translational velocity and (d) y-component of translational velocity for Case A (solid lines) and Case B (dashed lines).

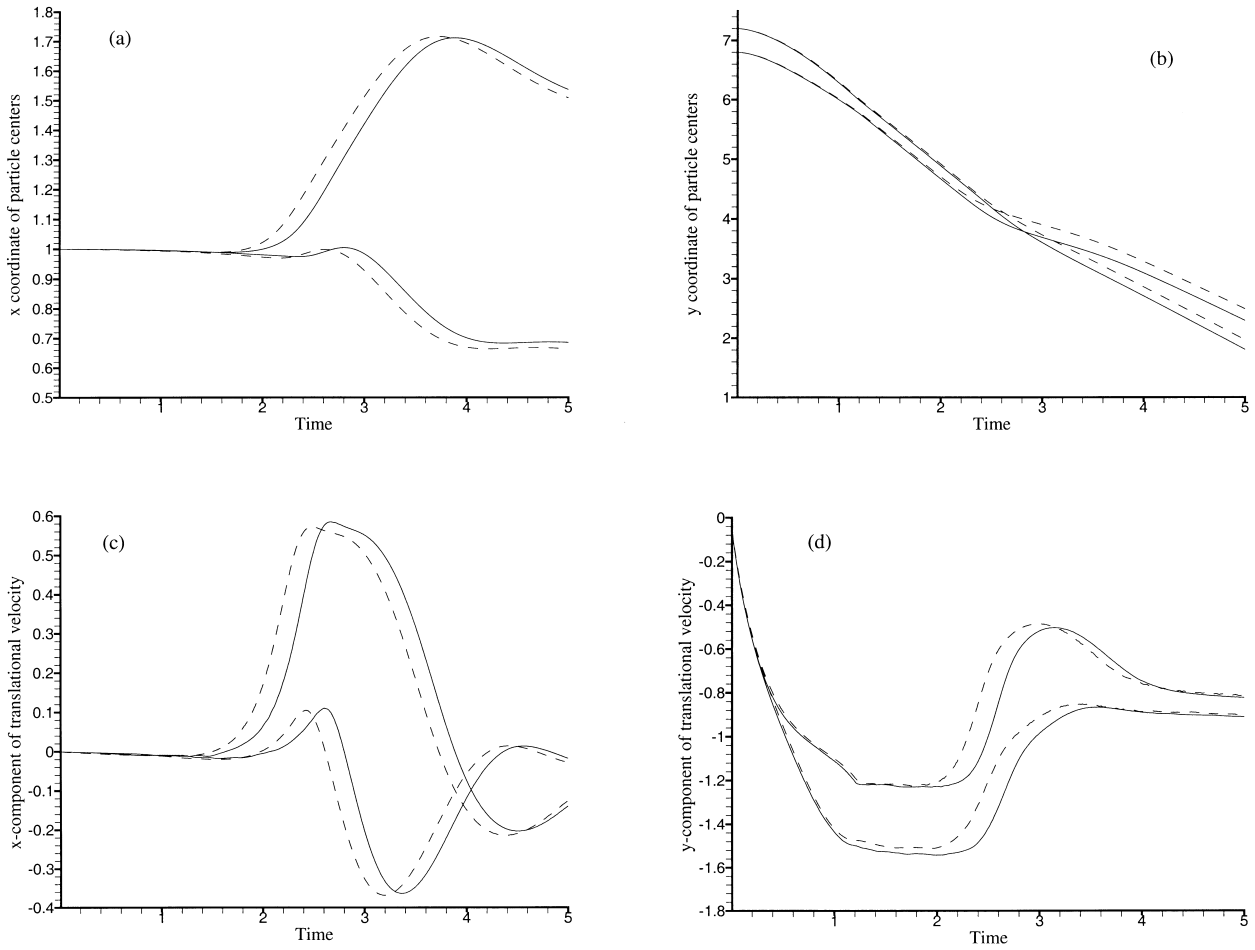

Fig. 3. Time history of (a) x-coordinate of particle centers, (b) y-coordinate of particle centers, (c) x-component of translational velocity and (d) y-component of translational velocity for Case B (dashed lines) and Case C (solid lines).

this observation. This simulation (Case A) has a velocity mesh size of 1/96 cm, pressure mesh size of 1/48 cm and the particle mesh size of 1/64 cm. The time step is 0.01 s. Results of another simulation (Case B) with a time step of 0.005 s are compared to those of Case A in Fig. 2. It is seen that the two cases are in good agreement until kissing and tumbling begins. This is because tumbling is essentially a breakup of an unstable configuration of the particle positions (Fortes et al., 1987). After tumbling is complete the particles continue to fall at locations away from the center of the channel at a constant speed. Fig. 2(d) shows that this terminal speed is the same in both the cases presented. There is greater agreement between the results if smaller time steps are used in the comparison. In Fig. 2 we wish to emphasize that the scheme gives good results even at comparatively larger time steps. We also note that the

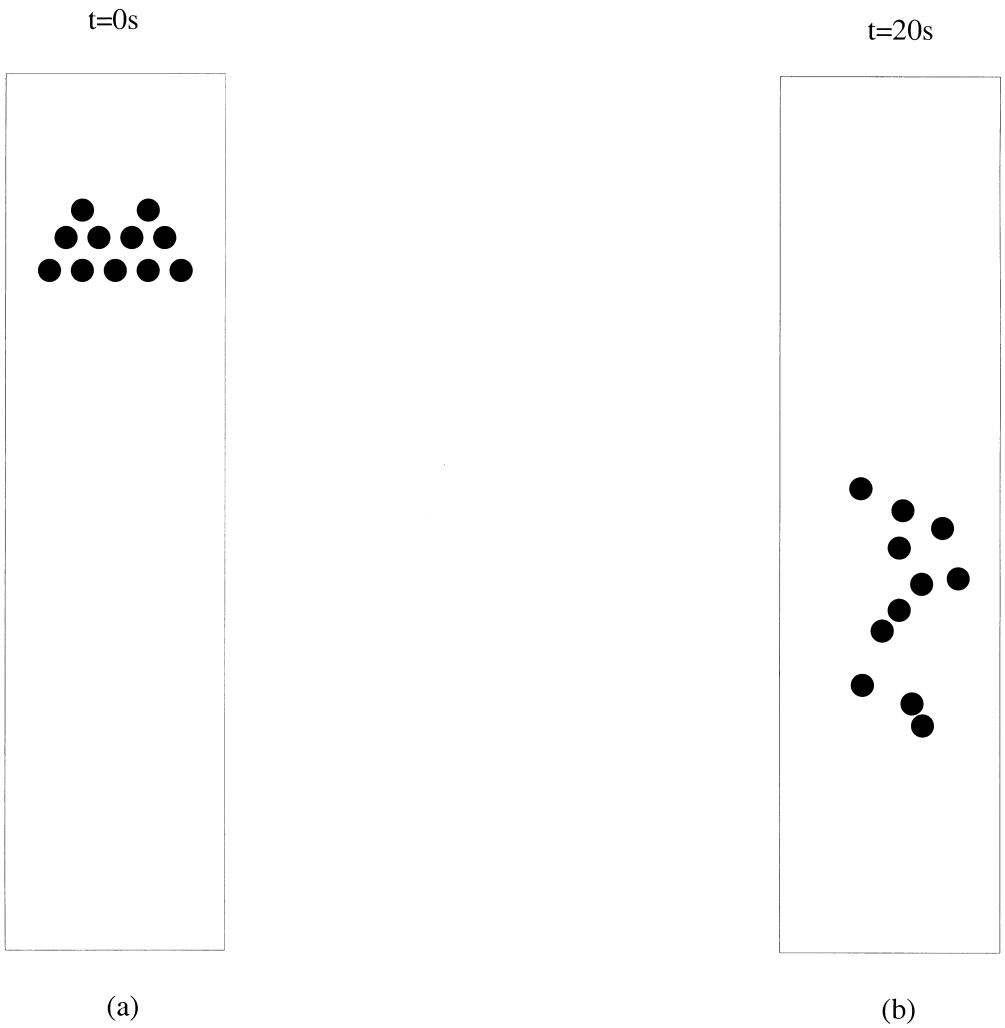

Fig. 4. Locations of eleven particles sedimenting in an Oldroyd B fluid at (a) $t = 0$ s and (b) $t = 20$ s.

overall qualitative behavior in both the cases is identical. This is important to ensure the same macroscopic behavior of the fluid particle mixture when the motion of large numbers of particles is simulated.

Results of Case B are also compared with another simulation (Case C) with a time step equal to 0.005 s, velocity mesh size of 1/144 cm, pressure mesh size of 1/72 cm and particle mesh size of 1/96 cm. Fig. 3 shows that these two cases are also in good agreement.

The above results are for the case of a Newtonian suspending fluid. The present code can also simulate the motion of particles in an Oldroyd B fluid. Particles falling in a viscoelastic fluid have a tendency to form chains (Joseph and Liu, 1993). This behavior was simulated by Huang et al. (1998) and Patankar (1997). To verify that the present code reproduces this behavior we consider sedimentation of eleven particles in a channel 2 cm wide and 8 cm tall. The initial positions of the particles are shown in Fig. 4(a). We consider an Oldroyd B fluid with a viscosity of 0.3 g/cm s, density of 1 g/cm^3 and relaxation time of 3 s. Density of the particles is 1.02 g/cm^3 and their radius is 0.1 cm. The time step is 0.005 s and the mesh size is same as that in Case C presented above. The Reynolds number ($= \rho_f V d/\eta$, where V is the particle velocity and d is the particle diameter) for this case is 0.167 and the Deborah number ($= V\lambda_r/d$, where λ_r is the relaxation time of the fluid) is 3.75. This results in a viscoelastic Mach number ($= \sqrt{Re\ De}$, where Re is the Reynolds number and De is the Deborah number) equal to 0.79 and the elasticity number ($= De/Re$) equal to 22.4. It was shown by Huang et al. (1998) that particles in a viscoelastic fluid tend to chain when Mach number is less than 1 and elasticity number is greater than 1. Fig. 4(b) shows the location of the particles at $t = 20$ s. There is a tendency to form chains which is in agreement with the previous results. More elaborate chain formation is expected from running this simulation for a long time in either a periodic channel or a calculation domain that moves with the particles. Such simulations will be focused in our future effort.

5. Conclusion

In this paper we have presented a new formulation of the Lagrange-multiplier-based fictitious-domain method for particulate flow. In this approach, rigid motion is enforced by requiring that the deformation rate tensor vanish at points occupied by rigid solids. This formulation leads to a field of Lagrange multipliers λ for rigid motion analogous to the way that pressure arises as a Lagrange multiplier for incompressibility. The new formulation is implemented by modifying the DLM code for two-dimensional particulate flows developed by Singh et al. (1999). The code gives results which agree with the original DLM approach when the densities do not match and with experiments.

The present algorithm requires no extra condition on the space of Lagrange multipliers when the fluid and particle densities match. In this approach the particle translational and angular velocities are not present in the combined equations of motion. This is especially convenient for extending the method to a three-dimensional case with irregularly shaped bodies where there is added complexity due to the nonlinear nature of the angular momentum equations.

Acknowledgements

We acknowledge the support from NSF under KDI/NCC grant NSF/CTS-9873236 and the University of Minnesota Supercomputing Institute. The authors are indebted to Todd Hesla, for his careful proofreading of the manuscript.

References

Bristeau, M.O., Glowinski, R., Priaux, J., 1987. Numerical methods for the Navier–Stokes equations. Comp. Phys. Rep 6, 73–187.

Feng, J., Huang, P.Y., Joseph, D.D., 1996. Dynamic simulation of the sedimentation of solid particles in an Oldroyd B fluid. J. Non-Newt. Fluid Mech 63, 63–88.

Fortes, A., Joseph, D.D., Lundgren, T.S., 1987. Nonlinear mechanics of fluidization of beds of spherical particles. J. Fluid Mech 177, 467–483.

Glowinski, R., Pan, T.-W., Hesla, T.I., Joseph, D.D., 1999. A distributed Lagrange multiplier/fictitious domain method for particulate flows. Int. J. Multiphase Flow 24, 755–794.

Glowinski, R., Pan, T.-W., Hesla, T.I., Joseph, D.D., Priaux, J., 1998. A fictitious domain method with distributed Lagrange multipliers for the numerical simulation of particulate flow. In: Mandel, J., Farhat, C., Cai, X.-C. (Eds.), Domain Decomposition Methods, vol. 10. American Mathematical Society, Providence, Rhode Island, pp. 121–137.

Hesla, T.I., 1991. The dynamical simulation of two-dimensional fluid/particle systems. Unpublished notes.

Hesla, T.I., 1995. Stress in a rigid body. Private communication.

Hesla, T.I., 1997. Partial reformulation of the Lagrange multiplier/fictitious domain method for particulate flows. Unpublished notes.

Hu, H.H., 1996. Direct simulation of flows of solid–liquid mixtures. Int. J. Multiphase Flow 22, 335–352.

Hu, H.H., Joseph, D.D., Crochet, M.J., 1992. Direct simulation of fluid particle motions. Theor. Comp. Fluid Dyn 3, 285–306.

Huang, P.Y., Feng, J., Hu, H.H., Joseph, D.D., 1997. Direct simulation of the motion of solid particles in Couette and Poiseuille flows of viscoelastic fluids. J. Fluid Mech 343, 73–94.

Huang, P.Y., Hu, H.H., Joseph, D.D., 1998. Direct simulation of the sedimentation of elliptic particles in Oldroyd B fluids. J. Fluid Mech 362, 297–326.

Huang, P.Y., Feng, J., 1995. Wall effects on the flow of viscoelastic fluid around a circular cylinder. J. Non-Newt. Fluid Mech 60, 179–198.

Johnson, A., Tezduyar, T., 1996. 3D simulation of fluid–particle interactions with the number of particles reaching 100. Research report 96-037, Army High Performance Computing Research Center, University of Minnesota.

Johnson, A., Tezduyar, T., 1997. Fluid–particle simulations reaching 100 particles. Research report 97-010, Army High Performance Computing Research Center, University of Minnesota.

Joseph, D.D., Liu, Y.J., 1993. Orientation of long bodies falling in a viscoelastic liquid. J. Rheol 37, 961–983.

Joseph, D.D., Lundgren, T.S., 1990. Ensemble averaged and mixture theory equations for incompressible fluid–particle suspensions. Int. J. Multiphase Flow 16, 35–42.

Patankar, N.A., 1997. Numerical simulation of particulate two-phase flow. Ph.D. thesis, University of Pennsylvania.

Singh, P., Joseph, D.D., Hesla, T.I., Glowinski, R., Pan, T.-W., 1999. Direct numerical simulations of viscoelastic particulate flows. J. Non-Newt. Fluid Mech., in review.